Colloid & Polymer Science Colloid Polym Sci 269:1099–1110 (1991)

Influence of nozzle geometry on polystyrene degradation in convergent flow

T. Q. Nguyen and H.-H. Kausch

Polymer Laboratory, Department of Materials Science, Swiss Federal Institute of Technology, Lausanne, Switzerland

Abstract: Polymer degradation is readily observed in flows where the extensional component surpasses the rotational component of the velocity gradient. This type of flow is conveniently obtained by pushing a liquid into a convergent channel across an orifice. Kinetics of chain scission is sensitive to subtle modification of the coil conformation, which in turn depends on the details of the pervading flow field. By changing the orifice diameter and the conical angle of the inlet, it is possible to modify the spatial distribution of the velocity gradient, and hence, the residence time of a fluid element in the high strain-rate region. Degradation yields, measured under θ-conditions in decalin by Gel Permeation Chromatography, showed a strong dependence on the fluid velocity at the orifice, but not on the magnitude of the strain-rate. This result is contrary to the common belief that assumes viscous friction, proportional to the strain-rate, is the determining factor for the scission rate of a bond under stress. Rather, experimental findings tend to indicate that the driving force for chain scission was provided by the energy accumulated in the coil during the flow-induced deformation process. The sharp propensity for mid-chain scission was maintained regardless of the nozzle geometry.

Key words: Convergent flow; nozzle geometry; mechanochemical degradation; polystyrene in decalin

I. Introduction

A number of stress-induced phenomena, such as chain orientation [1, 2], stress-induced diffusion [3, 4], and mechanochemical degradation [5, 6], have been observed in polymer flows with a large velocity gradient.

In order to study these processes, several types of equipment have been developed to create selected types of flow field under well-defined conditions: simple shear, pure shear, or elongational flows. Recent interest has been focused on the use of elongational flow as the one being capable of achieving a large degree of chain extension [7]. Within this latter category, convergent flow assumes a peculiar position due to its simple experimental realization and its frequent occurrence in several areas of rheology and engineering. Velocity fields in convergent flows have been investigated both for Newtonian and viscoelastic fluids under a variety of nozzle geometries ranging from abrupt contraction [8, 9] to diverse forms of conical, hyperbolic, or wedge-shape [10–12] tapered inlets.

In this study, we will examine some typical features of convergent flow with a particular emphasis on the processes of chain orientation and degradation. Axisymmertic flow across a narrow circular orifice will be used: such type of flow is capable of creating velocity fields with elongational strain-rates exceeding $4 \cdot 10^5\ s^{-1}$ and has proved to be particularly valuable for the investigation of mechanochemical degradation in solution.

*) Dedicated to Prof. W. R. Pechhold on the occasion of his 60th birthday

II. Experimental

Degradation apparatus

With the exception of the nozzle component, the degradation equipment is similar to that used in previous studies [5, 6, 13]. Two types of nozzle geometries have been selected: the abrupt contraction and the conical inlet (Fig. 1). Four different orifice diameters (0.35, 0.50, 0.68, and 1.00 mm) were used in the abrupt contraction flow; with the conical inlet, the orifice diameter was kept constant at 0.50 mm while the angle of the entrance was changed from 5° to 14°. The angle of the divergent outlet was maintained at 5°, except for one series of experiments (abrupt contraction with orifice diameter 0.50 mm) where it was changed to 14° to check for any detectable influence of the downstream region on the degradation yield.

All nozzles were made of stainless steel precisely machined by electroerosion; the inside geometry was controlled by using the silicon resin imprint technique. Orifice diameters were determined by a measuring microscope with an estimated precision of ± 5 μm.

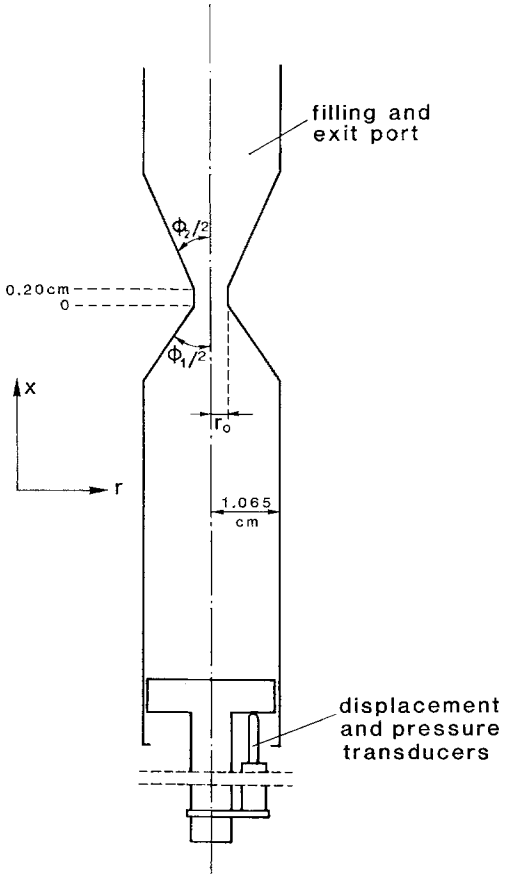

Fig. 1. Schematic representation of the degradation apparatus: $\phi_1 = 180°$ (abrupt contraction), 14° and 5° (conical inlet); $\phi_2 = 5°$ and 14°. (See text and caption of Fig. 4 for experimental values of the orifice diameter; figure is not drawn to scale)

Chemicals

Polystyrene is a Gel Permeation Chromatography (GPC) standard from Polymer Laboratories with a molecular weight at peak maximum of $1.08 \cdot 10^6$ and a ratio of weight-average to number-average molecular weight ($\overline{Mw}/\overline{Mn}$) < 1.05. The solvent, decalin, is a commercial mixture from Fluka AG containing 41% cis + 58% trans-decahydronaphtalene and 1% of tetrahydronaphtalene as determined by gas chromatography. It was vacuum-distillated prior to utilization.

Molecular weight determination

Molecular weight distributions of virgin and degraded polymer are determined by GPC on a Waters 150C equipped with a variable wavelength UV-detector (Perkin-Elmer 75C) and modified to permit data acquisition and processing on a personal computer (Hewlett Packard 9816). A set of Ultrastyragel columns (2×10^6 Å + 1×10^5 Å) was used for the separation.

Degradation conditions

All the degradation experiments are performed at 14.8 °C, which is the θ-temperature for the system decalin/PS. The polymer solution was pushed at constant velocity across the contraction and is collected for GPC analysis after a single passage. Both the piston velocity and the pressure drop were recorded for each run. No attempt was made to degas the solution: the dissolved oxygen, which acts as an efficient radical scavenger, is used to prevent any secondary reactions of the macroradicals formed during the degradation process.

Degradation is concentration dependent [14] down to the ppm level. To avoid this complication, the same polymer concentration of 5 ppm was used throughout the experiments. Such a low concentration prevented intermolecular entanglements and insured that each macromolecule acted effectively as an isolated entity.

III. Flow field analysis

The local molecular stress of a flexible polymer chain is directly related to the degree of coil extension by the stress–strain curve for a single chain [15]. Because molecular conformation depends on the details of viscous coupling between the monomer segments and the surrounding solvent molecules, a comprehensive flow-field analysis is a prerequisite for any attempt to understand the process of chain degradation in flow. Two quantities are particularly relevant in this respect: the magnitude and the spatial distribution of the velocity gradient inside the flow tube.

1. *Molecular extension and residence time*

A flexible polymer chain tends to be deformed from its equilibrium conformation in the presence of a velocity gradient. In terms of the linear elastic dumbbell model, it can be shown that the molecular coil is easiest to distort in a purely elongational flow [16]. De Gennes predicted a coil-to-stretch transition in elongational flow at a critical strain-rate $\dot{\varepsilon}_{cs}$ [17]:

$$\dot{\varepsilon}_{cs} \sim 0.5/\tau_z \,, \tag{1}$$

where τ_z is the longest relaxation time of the chain. This is given by Zimm's relation [18] in the non-free draining limit:

$$\tau_z = M\eta_s[\eta]/A_1 RT \,, \tag{2}$$

where η_s is the solvent viscosity, $[\eta]$ is the intrinsic viscosity, M is the polymer molecular weight, R is the molar gas constant, and T is the absolute temperature. The theoretical value for the dimensionless coefficient A_1 is dependent on the model, varying from 1.18 in Zimm's calculation [18] to 2.36 in some later papers [19]. Dynamic light-scattering measurements in the quiescent state [20] as well as birefringence measurements in opposed jet flows [7] give values for τ_z, which are somewhat lower than predicted from Eq. (2). In the absence of any definite experimental values pertinent to transient elongational flow, we prefer the original theoretical value of $A_1 = 1.18$ for the following discussion.

The strain-rate criterion given by Eq. (1) is a necessary, but not a sufficient condition for large chain extension, because the accumulated strain during the transit time in the region of high velocity gradient should exceed the maximum extension ratio λ_{max} of the considered coil:

$$\lambda_{max} = l_{max}/R_0 \,, \tag{3}$$

where R_0 is the rms end-to-end distance in the equilibrium state, and l_{max} is the maximum extended length of the polymer chain. For the $1.08 \cdot 10^6$ PS, l_{max} is equal to 2700 nm. $R_0 = 70$ nm is determined from intrinsic viscosity [21], $\lambda_{max} = 39$.

It is found that the degree of coil extension is sensitive not only to the strain rate, but also to the relative magnitude of the extensional flow component with respect to the rotational component. In terms of the velocity gradient, this means that the rate-of-strain tensor $\dot{\gamma} = \nabla v + (\nabla v)^T$ must be greater than the vorticity tensor $\omega = \nabla v - (\nabla v)^T$ in order to deform the molecular coil:

$$\|\dot{\gamma}\| > \|\omega\| \,. \tag{4}$$

With an increase in flow vorticity, nearly full chain extension is still possible, although at the expense of a rise in strain rate [16]. In the extreme case where vorticity and extensional rate are equal in magnitude, as encountered in simple shear flow, the coil rotates in the transverse velocity gradient and interacts successively for a limited time with the elongational and the compressional flow component during each turn. Because of the finite relaxation time of the chain [τ_z from Eq. (2)], it is believed that the macromolecule can no more follow these alternative deformations and remains in a steady deformed state above some critical shear rate ($\dot{\gamma}^*$) [19]. Simple shear flow is therefore much less efficient than elongational flow in promoting a large degree of coil extension:

$$\dot{\gamma}^* = \pi/\tau_z \,. \tag{5}$$

All of the previously described situations are actually encountered in a convergent flow: the flow field is purely elongational only along the symmetry axis; the vorticity component gains in importance with increasing distance from the centerline, and the flow becomes a simple shear next to the walls. The flow field remains, however, "predominantly elongational" in most parts of the tube at sufficiently high fluid velocity (sink flow). This flow field inhomogeneity can best be described by using the Giesekus criterion for local flow character [22], or it can be accounted for more quantitatively from a detailed kinetics analysis [23]. Experimental results and kinetics calculations showed that the experimentally determined spatially-average degradation yield is sufficient for a correct description of the degradation process. The most essential feature of convergent flow is the lack of a stagnation point: the flow is transient along any streamline, and chain extension is therefore limited before the point of rupture.

2. *Flow field calculations*

To investigate the effect of flow field on chain degradation, different nozzle geometries have been selected permitting to alter the experimental flow field within some certain limits. All the flow-field

calculations reported in this section and in the ensuing discussion are performed with the flow simulation program POLYFLOW [24] on an APOLLO DN-3000 station. We applied the hypothesis that the polymer solution was incompressible and behaved as a Newtonian fluid with a density of $0.890\,g\cdot cm^{-3}$ and a shear-independent viscosity $\eta_s = 2.77$ mPa · s. At the present state of dilution (5 ppm), it is probably a fair approximation to neglect viscoelasticity at the macroscopic scale. Even if some non-Newtonian effects could already be observed at the ppm level like in drag reduction or in the "bathtub" vortex [25], the present studies suggest that it plays only a secondary role for chain degradation. At the molecular level, the energy to distort the molecular coil should be taken from the surrounding fluid; as a result of this mutual coupling, it is expected that the velocity field at the vicinity of a stretching chain will be somewhat different from the bulk macroscopically-average flow field.

a) With abrupt contraction flow, most of the fluid acceleration occurred within ~ 1 orifice diameter in front of the orifice and gives the characteristic spike-like shape for the longitudinal strain-rate distribution. In Fig. 2, we have plotted the elongational strain-rate along the centerline for different orifice diameters. As usual in this type of representation, the coordinates are made dimensionless by dividing the variable under consideration with a conjugated parameter (the subscript "'" indicates the dimensionless coordinate, r_0 is the orifice diameter, and $\bar{v}_0$ is the volumetric-average fluid velocity at the orifice) so that

$$x' = x/r_0 \,, \tag{6}$$

$$v'_x = v_x/\bar{v}_0 \,, \tag{7}$$

and

$$\dot{\varepsilon}'_{xx} = \delta v'_x/\delta x' = \dot{\varepsilon}_{xx}/(\bar{v}_0/r_0) \,. \tag{8}$$

Another quantity of importance for determining residence time is dimensionless time (t') defined as

$$t' = t/(r_0/\bar{v}_0) \,. \tag{9}$$

Within computational errors, all the calculated strain-rates for the different orifice diameters are exactly superposable onto a single curve with a maximum $\dot{\varepsilon}_{xx}(\max)$ given by

$$\dot{\varepsilon}_{xx}(\max) = 0.56\cdot\bar{v}_0/r_0 \,. \tag{10}$$

For a given fluid velocity $\bar{v}_0$, the strain-rate distribution function reaches its highest value with the smallest orifice diameter, accompanied by a concomitant decrease in the spatial extension (Figs. 2 and 3).

b) Conical inlet

Abrupt contraction flow is characterized by a recirculation vortex surrounding the nozzle, which increases in importance with viscoelastic fluids. To avoid this problem, it is common to use a conical inlet instead of the abrupt contraction: it has been shown experimentally that the recirculation eddy could be suppressed by using a tapered inlet with a

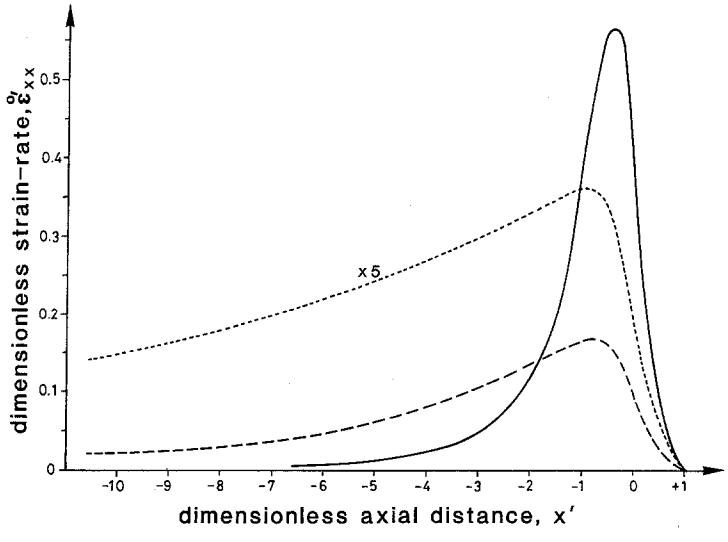

Fig. 2. Entrance elongational strain-rate ($\dot{\varepsilon}'_{xx}$) calculated along the centerline of the flow tube for the different nozzle geometries. (The origin of the abscissae is taken at the orifice entrance.) (——) abrupt contraction, (– – –) 14° conical inlet, (- - -) 5° conical inlet

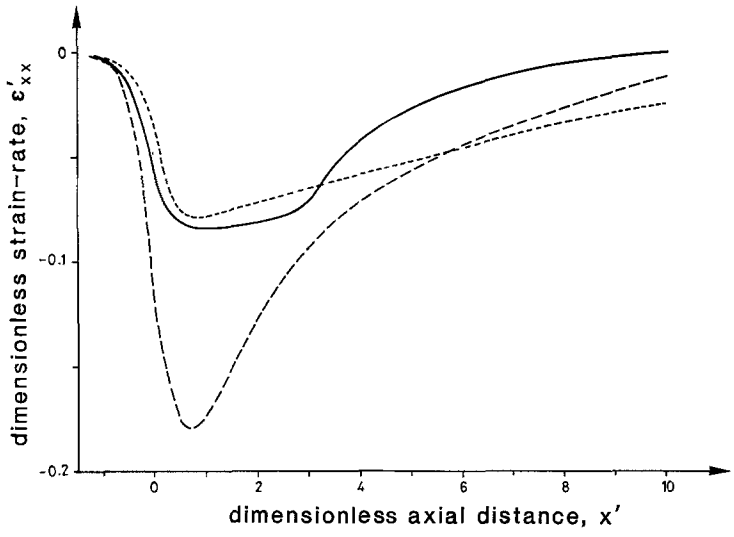

Fig. 3. Compressional elongational strain-rate ($\dot{\varepsilon}'_{xx}$) calculated along the centerline of the flow tube for the different exit geometries. (The origin of the abscissae is taken at the location of the divergent outlet.) (——) free jet ($\bar{v}_0 = 35\ \mathrm{m \cdot s^{-1}}$), (– – –) 14° conical outlet, (- - -) 5° conical outlet

conical angle less than 40° [8]. In the present study, using a conical inlet has the added advantage of providing a simple means of modifying the velocity gradient distribution by a proper selection of the entry angle (Fig. 2). Compared with the abrupt contraction at an identical flow-rate and orifice diameter, the conical entrance provides an increase in spatial distribution of the strain-rate distribution function by a factor of 3 with the 14° inlet up to a factor of 8 with the 5° angle. This increase in width is accompanied by a decrease of roughly the same factor in the amplitude of the fluid strain-rate:

$$\phi_1 = 14°, \quad \dot{\varepsilon}_{xx}(\max) = 0.17 \cdot \bar{v}_0/r_0 \tag{11}$$

and

$$\phi_1 = 5°, \quad \dot{\varepsilon}_{xx}(\max) = 0.07 \cdot \bar{v}_0/r_0\ . \tag{12}$$

c) Flow field at the outlet

A divergent outlet was used to suppress backflow of the solution, and to prevent shear degradation from high shear buildup at the walls (Fig. 3). From the Stokes' reversibility principle, it is predicted that the streamline pattern of an incompressible Newtonian liquid will remain unchanged when the flow direction is reversed. At a given conical angle, the extensional strain-rate in the convergent flow becomes a negative compressional strain-rate at the divergent exit of practically the same amplitude, as found in the former situation. Strain-rates of such a magnitude could be sufficient to induce chain scission so that the geometry of the exit should be designed with the same care as for the entrance to avoid uncontrolled degradation. To verify whether any observed degradation could occur in the exit section of the tube, we used two different divergent angles of 5° and 14° for the outlet. In yet another series of experiments, the polymer solution was allowed to spring freely into a large reservoir after the orifice. Here we take advantage of the capability of the POLYFLOW program to handle the presence of a free surface. The results showed a contraction of the free jet after the exit following a rearrangement of the velocity profile. The velocity gradient is dependent upon the Reynolds number in the free jet, and the dimensionless representation is strictly speaking not applicable in this case.

Although the exit-flow fields were markedly different in these situations, the measured degradation yields were identical. This supports the idea that most of the degradation effectively occurs in the high strain-rate region in front of the orifice.

d) Role of turbulence

Turbulence is known to be a source of polymer degradation during drag reduction. In pipe flow, the transition from laminar to turbulent regime occurs when the dimensionless Reynolds number

$$Re = 2\bar{v}r\rho/\eta_s \tag{13}$$

is greater than 4000. In the vicinity of the orifice ($r \sim r_0$), the values of Re relevant to the present experimental conditions are all much greater than 4000, and turbulence could well be induced in the narrowest section of the tube. We believe, how-

ever, that it will not affect the degradation results in convergent flow for one good reason. During a previous investigation on the effect of solvent viscosity [21], the degradation yields were measured systematically over a large range of Reynolds numbers extending from $2 \cdot 10^2$ to $2 \cdot 10^5$. No significant deviation from the observed trend was detected around the critical Re of 4000. In the absence of external disturbances, laminar flow with a Reynolds number in excess of 40 000 has been observed in a smooth tube. It could be that the time scale in transient convergent flow is simply too short to promote the development of turbulent eddies.

IV. Results and discussion

Chain scission through frictional loading model

The proportion of polymer molecules degraded after a single passage across the orifice was determined by Gel Permeation Chromatography. Bimodal distribution of the GPC traces reflected the precision of the midchain scission, which remained extremely sharp regardless of the nozzle geometry (standard deviation $\sigma = 7\%$). In conformity with our previous publications [6, 13], we have reported the degradation yields as a function of strain rate for different nozzle geometries (Fig. 4). The fluid strain rate that marks the onset of chain fracture is denoted as $\dot{\varepsilon}_f$. Due to the molecular weight distribution in the undegraded polymer, $\dot{\varepsilon}_f$ refers to the highest molecular weight present in the sample. The effective $\dot{\varepsilon}_f^*$ for the molecular weight at peak maximum ($1.08 \cdot 10^6$) is slightly lower than $\dot{\varepsilon}_f$ and corresponds to a scission yield of $\sim 7\%$ on the degradation curves of Fig. 4 [23]. The most apparent feature from the reported data is a lack of any coincidence between the critical strain rate for chain fracture ($\dot{\varepsilon}_f$) and the fluid strain rate ($\dot{\varepsilon}$). This result is in clear disaccord with the model of chain scission through frictional loading (also known as the thermo-mechanical activation model). In this model, mechanochemical degradation is treated as a chemical process promoted by thermal fluctuations in which the activation energy has been reduced from its equilibrium value by the presence of mechanical stress. The rate of chain scission is given by an Arrhenius-type equation [26] and becomes appreciable only when the locally applied stress approaches the breaking strength (F_b) of the bond under consideration. Overall, the molecular chain behaves like a macroscopic string with a mechanical strength given approximately by the maximum of the derivative of the Morse potential (ca 4–6 nN for a C–C bond) [15, 27]. In dilute polymer solutions, the transmission of force in a stationary situation is thought to be provided by the viscous friction between polymer segments and flowing polymer molecules. According to the Stokes' law, this hydrodynamic drag force is proportional to the relative velocity between a monomeric unit and the bulk fluid velocity, and hence, to the fluid strain rate $\dot{\varepsilon}$. The observed dispersion of

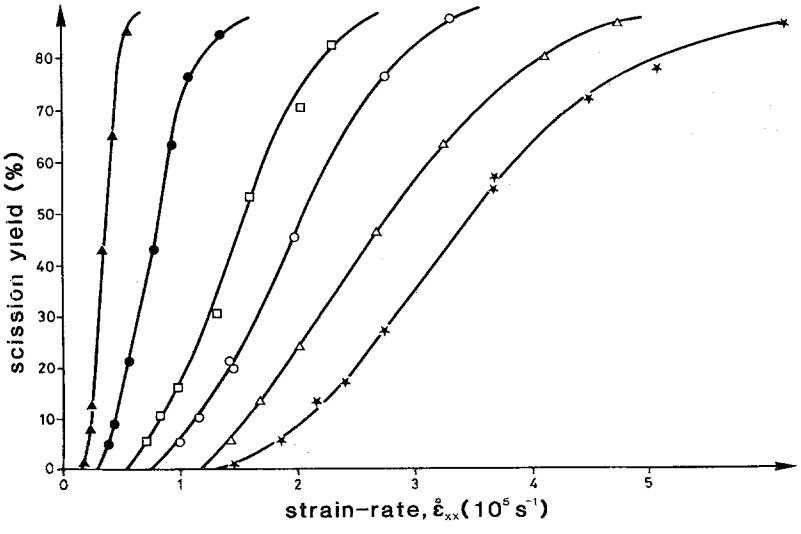

Fig. 4. Degradation yield as a function of maximum entrance strain-rate ($\dot{\varepsilon}_{xx}$) for different nozzle geometries: (★) abrupt contraction, $r_0 = 0.175$ mm; (△) abrupt contraction, $r_0 = 0.25$ mm; (○) abrupt contraction, $r_0 = 0.34$ mm; (□) abrupt contraction, $r_0 = 0.50$ mm; (●) 14° conical inlet, $r_0 = 0.25$ mm; (▲) 5° conical inlet, $r_0 = 0.25$ mm

the degradation yields in Fig. 4 suggests that the scission event is not controlled by the frictional stress at the point of fracture, because the same molecular breaking force must be involved regardless of the nozzle geometry. A possible explanation to reconciliate with the frictional model would be to use a nozzle-dependent coil-expansion factor. The latter quantity will be discussed subsequently in more detail for two reasons: 1) results of flow field calculations show that the residence time, one of the key parameters for determining the degree of coil expansion, also changes with the nozzle geometry (Fig. 2); 2) $\dot{\varepsilon}_f^*$ varies with M^{-1}, indicating the scission of a non-extended coil [13].

It is usual to model the deformed coil as an elongated cylinder of length L and diameter d. Results of slender-body hydrodynamics give a parabolic distribution of stress along the body with a maximum at mid-coil equal to

$$F_{max} = [(2\pi/\ln(L/d)] \cdot \eta_s \cdot \dot{\varepsilon} \cdot L^2/8 \,. \qquad (14)$$

The probability between F_{max} and $\dot{\varepsilon} \cdot L^2$ could be used as an argument to rationalize the experimental results, because a more expanded coil could also be fractured at a lower strain rate. More detailed analysis showed, however, several drawbacks of the proposed model.

a) Polymer dynamics results, supported by rheology measurements, confirm that the molecular coil starts to be deformed only at $\dot{\varepsilon} > \dot{\varepsilon}_{cs}$ ("cs" referring to the coil-to-stretch transition) and slowly retracts at $\dot{\varepsilon} < \dot{\varepsilon}_{sc}$. Due to an hysteresis effect, the critical strain-rate ($\dot{\varepsilon}_{sc}$) for the stretch-to-coil transition is smaller than $\dot{\varepsilon}_{cs}$ by an amount that depends on the degree of chain extension. Its exact value is irrelevant for the present purpose, because the fluid velocity v_{sc}, corresponding to $\dot{\varepsilon}_{sc}$, is always close to v_x(max) following the sharp decrease of $\dot{\varepsilon}_{xx}$ behind the orifice (Fig. 5). From Eqs. (1) and (2), the critical strain-rate $\dot{\varepsilon}_{cs}$ for the PS sample calculated with the available experimental data [21] is found to be equal to 11 400 s^{-1}. At a given average fluid velocity $\bar{v}_0$, the amplitude of $\dot{\varepsilon}_{xx}$ is highest with the abrupt contraction and with the smallest orifice diameter (Fig. 5); therefore, $\dot{\varepsilon}_{cs}$ would also be reached at a lower value of the axial fluid velocity denoted by v_{cs} in Fig. 5. The maximum degree of chain extension is bound by the ratio $\lambda_{fl} = v_{sc}/v_{cs} \sim \bar{v}_0/v_{cs}$ (with $\bar{v}_0 \sim 35$ m·s^{-1}); this upper limit will be reached only in case of an affine deformation of the coil with the surrounding fluid element. The ratios λ_{fl}, obtained from the computed axial velocity distribution, are given below for the different nozzle geometries and show that the achievable degree of coil expansion actually goes in a direction contrary to the expectation:

1) abrupt contraction, $r_0 = 0.0175$ cm, $\lambda_{fl} = 19.3$,
2) abrupt contraction, $r_0 = 0.025$ cm, $\lambda_{fl} = 14.1$,
3) abrupt contraction, $r_0 = 0.034$ cm, $\lambda_{fl} = 11.4$,
4) abrupt contraction, $r_0 = 0.050$ cm, $\lambda_{fl} = 8.7$,
5) 14° conical inlet, $r_0 = 0.025$ cm, $\lambda_{fl} = 3.3$,
6) 5° conical inlet, $r_0 = 0.025$ cm, $\lambda_{fl} = 1.6$.

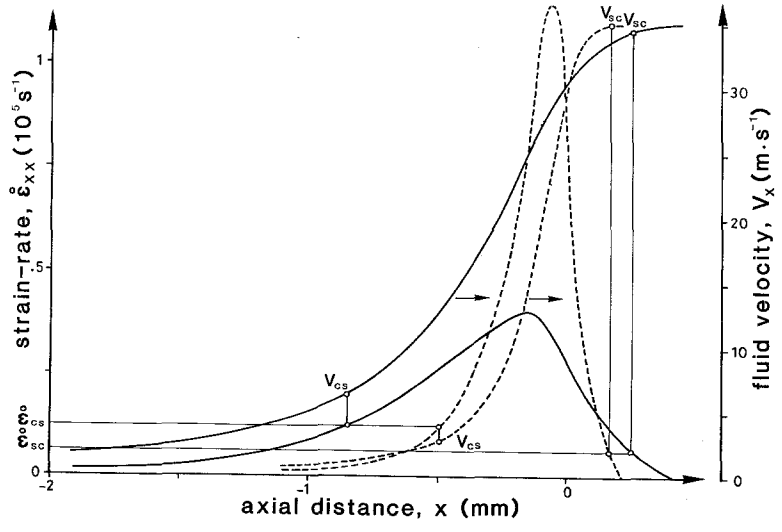

Fig. 5. Relation between the degree of chain extension and the axial velocity profile in abrupt contraction flow (axial velocity curves: right scale ordinate). (– – –) $r_0 = 0.175$ mm, (——) $r_0 = 0.50$ mm

The results obtained with the 5° inlet have several interesting implications that may grant further investigations:

- The estimated maximum of possible coil extension at the point of fracture is a mere factor of 1.6. Following the discussion in Sect. III-1 and depending on the exact value of A_1 in Eq. (2), this factor could be even lower than the quoted value. It is then legitimate to question whether a polymer chain can still be degraded even if the fluid strain-rate is below the critical value to induce a coil deformation. The correctness of this assertion could be verified by using a less viscous solvent, such as ethyl-methyl ketone. From a previous publication [28], it was shown that $\dot{\varepsilon}_f \sim \eta_s^{-0.25}$, whereas $\tau_z \sim \eta_s^{+1}$; by reducing η_s, a point will be reached where the relation $\dot{\varepsilon}_{cs} \sim 0.5/\tau_z < \dot{\varepsilon}_f$ would no longer be verified.
- By gradually reducing the angle ϕ_1 of the conical inlet, it is possible to make a smooth transition from an elongational flow to a simple shear flow. At some stage, it is predicted that the degradation yields will drop sharply, because little chain scission is expected in capillary flow.

b) In a pioneering experiment, Smith et al. [2] have determined the degree of coil expansion (λ) in abrupt contractional flow by light scattering. Their reported value of $\lambda < 4$ showed a limited degree of coil expansion for PS with molecular weights ranging from $1.7 \cdot 10^6$ to $4.8 \cdot 10^6$. Indirect evidence obtained from the concentration dependence of the scission yields also tends to indicate a similar degree of coil expansion under present experimental conditions [14]. Replacing the different parameters of Eq. (14) by their approximate values gives $F_{max} = 1 \cdot 10^{-11}$ N, which is over 2 orders of magnitude below the actual breaking strength of the C–C bond.

These facts tend to indicate that the frictional model for chain scission is inadequate to explain degradation in transient elongational flow, and an alternative model is now proposed.

Critical energy model

Figure 4 reveals an inverse dependence of $\dot{\varepsilon}_f$ on orifice diameter. The existence of a similar relationship with the fluid strain rate (Fig. 2) suggested that a better correlation could be obtained by reporting the degradation yields as a function of average orifice velocity for the different nozzle geometries. Figure 6 shows effectively that all the degradation for the abrupt contraction as well as for the conical inlets can be superimposed onto a single curve. Although some dispersion is still present, it is considerably reduced as compared to the plots of Fig. 4. In part, this can be accounted for by the imprecision in the determination of the orifice diameters.

In convergent flows, flow-rate and entrance pressure drop are two dependent variables whose relationship is well-documented both theoretically and experimentally for different nozzle geometries [28].

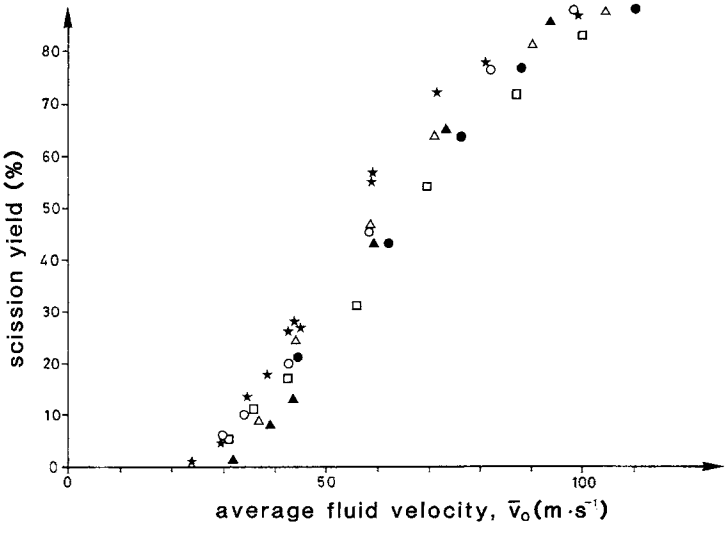

Fig. 6. Degradation yield as a function of volumetric average fluid velocity at the orifice ($\bar{v}_0$). (Same symbols are used as in Fig. 4)

Instead of reporting the degradation yields as a function of $\bar{v}_0$, the other alternative would be to report the same results as a function of the entrance pressure drop P_{ent} (Fig. 7): a weak increase in degradation efficiency with decreasing orifice diameter is observed with this type of plot and may have some importance in polymer flow across porous media. The most remarkable feature is certainly the perfect coincidence between the data points obtained with the conical inlets and with the abrupt contraction of identical orifice diameters. Although the velocity fields are quite different in each case, the chains break with identical efficiency at a given pressure drop (or energy input): such a coincidence is certainly not fortuitous and conceals a deeper underlying mechanism that still needs to be sought. The shape of the curves in Fig. 7 satisifes the intuitive idea that the number of broken bonds should increase with the total energy input into the flowing system; it also suggests the existence of a critical level of energy, corresponding to $P_{ent} \simeq 1$ atm or $\bar{v}_0 = 35\ \mathrm{m \cdot s^{-1}}$, below which no degradation occurs regardless of the nozzle geometry.

From these experimental results, it is tempting to speculate that the principal factor governing the fate of a stressed macromolecule is the amount of elastic energy (E_{el}) stored in the deformed chain. The energy stored in the chain evidently must be strongly related to the energy dissipated within the fluid volume element just circumscribing the molecular coil. This energy E_s could be obtained from the rate of energy dissipation (J) equal to the product of fluid elongational stress ($\tau_{xx} - \tau_{rr}$) and fluid elongational strain-rate ($\dot{\varepsilon}_{xx}$):

$$J = \int_V (\tau_{xx} - \tau_{rr}) \cdot \dot{\varepsilon}_{xx}\, dV \ . \tag{17}$$

Alternatively, energy could be compared with the average tension $F(r)$ in the stretched coil:

$$E_{el} = \int_{R_0}^{r} F(r')\, dr' \ . \tag{18}$$

In the freely jointed bead-spring model, $F(r)$ is approximated by a Hookean force law at modest extension ratio ($\lambda < 4$) of the molecular coil and Eq. (18) becomes:

$$E_{el} = 3/2\, kT \cdot \lambda^2 \ . \tag{19}$$

E_{el} calculated from Eq. (19) at $\lambda = 4$ is equal to $1 \cdot 10^{-19}$ J/molecule; this quantity is much below the dissociation energy U_0 of the C–C bond, which is $5.7 \cdot 10^{-19}$ J/bond or $342\ \mathrm{kJ \cdot mol^{-1}}$ for polystyrene. It can be assessed, however, from the occurrence of chain scission that the actual value for E_{el} must be significantly larger than that given by Eq. (19). The same conclusion was drawn previously under other circumstances:

a) It was determined that the elongational stress [Eq. (17)] in convergent sink flow of dilute polymer solutions surpasses the value predicted with the Gaussian dumbbell [10]. The discrepancy with theoretical predictions was interpreted in terms of the "yo-yo" model. Regardless of the validity of the

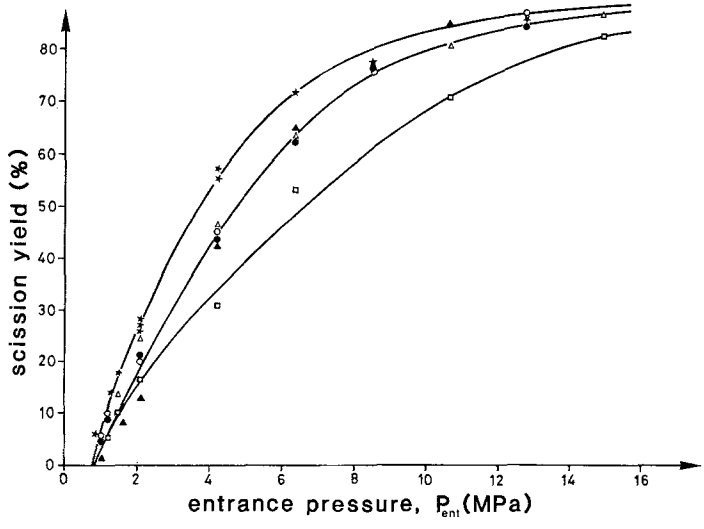

Fig. 7. Degradation yield as a function of experimental entrance pressure drop. (Same symbols are used as in Fig. 4). Curves for $r_0 = 0.25$ mm and $r_0 = 0.34$ mm are experimentally indistinguishable

model, the point is that the dissipated energy is much greater than could be accounted for by the rubber elastic Hookean spring.

b) The bead-spring model assumes that the polymer is completely limp except for the entropic spring force to resist stretching. At high strain-rates, it is expected that the above model is indeed a poor approximation to the dynamics of real molecular chains. In a preceding publication [21], it was established that the solvent viscosity has only a weak influence on the degradation yield and the results were interpreted in terms of the internal viscosity of the molecular coil. It is generally agreed that internal viscosity stems mainly from two molecular mechanisms: the first was noted by Kuhn one-half century ago [29] and comes from the hindered rotation around the skeleton bonds; the resulting force counteracts the deformation process and is strain-rate and molecular-weight dependent. The second effect, proposed by Cerf [30], takes its origin from the intramolecular friction between the sliding segments and depends principally on the rate of extension [31].

It is usual to model the force law for a dumbbell with internal viscosity as a Hookean spring with a linear dashpot in parallel [32]: $F(r)$ is now strain-rate dependent and increases with the average rate of extension of the coil. Within the range of high strain-rates prevalent to the process of chain degradation, $F(r)$ and hence E_{el} could be much higher than predicted by the simple Hookean law. Even at modest extension ratio, it could be seen that the energy accumulated within the coil is sufficient to break the covalent bond, whereas the computed stress at the same deformation stage is not.

The notion of a critical energy for bond rupture is not new in itself and has periodically surfaced over the years in the field of mechanochemical degradation. From the standpoint of thermodynamics, the essential quantity governing the course of a chemical reaction is the chemical potential of the system or, in the case of interest, the free energy storage within the molecular coil. This quantity is, unfortunately, difficult to evaluate and most models on mechanochemical degradation relied on some sort of empirical relationship existing between the rate of chain scission and an experimental variable that could be directly measured, such as, for instance, the rate of mechanical energy input. To rationalize degradation results during capillary extrusion of concentrated polyisobutylene solutions, Bestul [33] assumed that a polymeric system under shear reaches a pseudo-equilibrium steady-state condition with respect to the temporary stored energy contributed by the shear field. By analogy with kinetics for thermal activation, the following expression was derived for the probability that a bond attains the activation energy necessary to be ruptured:

$$P = 1/(kT - aJ)\,[kT \cdot \exp(-E^*/kT) - aJ \cdot \exp(-E^*/aJ)]\,. \quad (20)$$

In this equation, E^* is the mechanical activation energy for bond rupture (approximated as the bond-dissociation energy U_0), J is the rate of application of shear energy that equals the shear rate times the shear stress, and a is a coefficient having the dimension of time (a is constant for a given shearing condition but increases with the polymer molecular weight). The product aJ gives the average amount of applied shear energy, which is temporarily stored in bonds.

Under conditions where the thermal energy contribution can be neglected, the rate for shear degradation was given as:

$$-dN/dt = k_c N = B\exp(-E^*/aJ)\,, \quad (21)$$

where N is the number of undegraded polymers at time t.

By plotting $\log k_c$ as a function of $1/J$, it was found that all the experimental points could be fitted onto straight lines, in accord with the prediction from Eq. (21) [33].

More recently, in a series of intriguing experiments, Wolf et al. [34] found that moderately concentrated polymer solutions in laminar shear flow do not degrade as long as the quality of the solvent remains high; with decreasing temperature, the rate of chain rupture increases steeply in the vicinity of the demixing point and then decreases again. In order to explain this complex behavior, Wolf [35] proposed the formation of "grip points" along the chain: degradation will be observed only if the amount of stored energy per grip point is superior to the activation energy E^* for bond scission. The maximum in the degradation curve as a function of temperature could now be envisioned as a balance between the reduction in coil volume and the increase in stored energy per macromolecule.

Although no intermolecular entanglements could be formed at the low polymer concentration

used in the present investigation, the possibility of long-range *intra*molecular contact points and of local "kinetic rigidity" implicit to the concept of "internal viscosity" must be admitted; under these conditions, stress accumulation becomes possible and leads to bond rupture in a similar way as through the "grip points" considered by Wolf.

The problem remains how the chain knows its center during the process of loading to explain the sharp midchain scission invariably observed. Already from purely geometrical arguments, it could be assessed that bond rupture should be non-random: because the chain ends are more mobile than the inner parts of the polymer, they should be able to relieve stresses more readily; bond scission, if it occurs, should be found preferentially near the middle by reason of symmetry. Calculations of the stress distribution in an undeformed coil under elongational flow indeed confirmed this intuitive argument [36]. The estimated standard deviation $\simeq 0.3$ is, nevertheless, much greater than the experimental values, which varied from 0.04 in the good solvent methyl-naphtalene to 0.07 in the θ-solvent decalin.

IV. Conclusion

For almost a decade, it was predicted and verified that flexible macromolecules in solution could be stretched and fractured in a highly extended state. The sharp midchain scission, as well as the dependence of $\dot{\varepsilon}_f$ on $\eta_s^{-1} \cdot M^{-2}$ found by Keller and Odell [37] are correctly explained with the use of the thermo-mechanically activated model for bond rupture under stress. Ultimate mechanical properties of highly oriented polymer chains in bulk are also accurately predicted with the above-mentioned model, leaving little doubt to its ability to explain physical properties of polymer molecules in the fully stretched state.

In a series of experiments performed in our laboratory [6, 13, 21], it was shown that polymer chains in a partly uncoiled state behave in a quite different and intricate way from chains in a highly oriented state. The following experimental facts cannot be explained by the model of fully extended frictionally loaded chains:

- $\dot{\varepsilon}_f \simeq M^{-1}$,
- $\dot{\varepsilon}_f \simeq \eta_s^{-0.25}$,
- Degradation yield is a fairly unique function of (average) fluid velocity almost independent of differences in elongational strain rate introduced by nozzle geometry,
- Degradation yield is a fairly unique function of entrance pressure drop and thus, of energy introduced into the deformed liquid volume element.

In order to satisfy one or the other of the above facts, three hypotheses have been discussed:

1) The flow is not laminar but turbulent and the flow pattern is not predictable from $\bar{v}_0$ or an apparent $\dot{\varepsilon}_f$.
2) Coil dimensions and local viscosity depend on strain rate and nozzle geometry.
3) The affinely deforming coil stiffens and is capable of storing appreciable amounts of elastic energy.

So far, none of these hypotheses can fully be proven or disproven. All analyses of the occurrence of turbulent flow show, however, that No. 1 is the least likely explanation. The same is true for the second hypothesis, which necessitates complicated deviations from fundamental behavior *without* explaining the sharpness of midchain scission. In the authors' opinion the third hypothesis is the most probable one: in an affinely deforming liquid, chains are almost statically loaded from the surface of the circumscribed volume element. Internal relaxation of the chain relieves some of the axial chain stresses and contributes to the small ($\lambda = 1.6$) to moderate ($\lambda = 19.3$) elongation. By inter-segmental interaction, stresses are transferred from the surface to the center of the coil. It remains to be shown why the "center of the coil" coincides to such precision with the "center of the chain."

Although significant insight into the process of bond rupture has been gathered from the above studies on degradation kinetics, it remains desirable at this stage to carry out further experiments at a more microscopic level, for example by determining the degree of coil expansion as a function of strain-rate inside the flow tube. Designing an experiment capable of providing information on the coil geometry in flow is challenging in many respects (high velocity at the orifice, small sensitivity due to the low concentration involved, inhomogeneity within the flow region). It seems, however, this effort is necessary for a better comprehension of this phenomenon.

Acknowledgements

Frequent discussions with A. Keller and J. Odell and financial support from the Swiss National Science Foundation are gratefully acknowledged.

References

1. Keller A, Mackley MR (1974) Pure Appl Chem 39:195
2. Smith KA, Merrill EW, Peebles LH, Banijamali SH (1975) Polymères et Lubrification, Colloques Intern du CNRS, Paris 233:341
3. Akay G (1982) Polym Eng Sci 22:798
4. Jhon MS, Sekhon G, Armstrong RC (1987) Adv Chem Phys 66:153
5. Merrill EW, Leopairat P (1980) Polym Eng Sci 20:505
6. Nguyen QT, Kausch HH (1986) Colloid Polym Sci 264:764
7. Pope DP, Keller A (1978) Colloid Polym Sci 256:751
8. Nguyen H, Boger DV (1979) J Non-Newt Fluid Mech 5:353
9. Viriyayuthakorn M, Caswell B (1980) J Non-Newt Fluid Mech 6:245
10. Ryskin G (1987) J Fluid Mech 178:423
11. Gatski TB, Lumley JL (1978) J Fluid Mech 86:623
12. Crater DH, Cuculo JA (1983) J Polym Sci Polym Phys Ed 21:2219
13. Nguyen QT, Kausch HH (1988) J Non-Newt Fluid Mech 30:125
14. Nguyen QT, Kausch HH (1990) results to be published
15. Kausch HH (1987) Polymer fracture, 2nd Ed. Springer Verlag, Berlin-Heidenberg, p 129
16. Leal LG (1985) In: Rabin Y (ed) Polymer-flow interaction. American Institute of Physics, New York, p 5
17. De Gennes PG (1974) J Chem Phys 60:5030
18. Zimm BH (1956) J Chem Phys 24:269
19. Layec-Raphalen MN, Wolff C (1976) J Non-Newt Fluid Mech 5:463
20. Nicolai T, Brown W, Johnsen R (1989) Macromolecules 22:2795
21. Nguyen QT, Kausch HH (1990) Macromolecules 23:5137
22. Giesekus H (1962) Rheol Acta 2:122
23. Nguyen QT, Kausch HH (1989) Makromol Chem 190:1389
24. Polyflow SA, Polyflow, a finite element program for calculating viscous and viscoelastic flows. Polyflow SA, Louvain-la-Neuve, Belgium
25. Bird RB, Armstrong RC, Hassager O (1987) Dynamics of polymeric liquids, 2nd Ed. John Wiley Sons, New York, Toronto, 1:82
26. Zhurkov SN, Korsukov VE (1974) J Polym Sci Polym Phys Ed 12:385
27. Boudreaux DS (1973) J Polym Sci Polym Phys Ed 11:1285
28. Tanner RI (1988) Engineering rheology, Rev. Ed. Clarendon Press, Oxford, p 329
29. Kuhn W, Kuhn H (1946) 29:609
30. Cerf R (1957) J Polym Sci 23:125
31. De Gennes PG (1977) J Chem Phys 66:5825
32. Bird RB, Armstrong RC, Hassager O (1987) Dynamics of polymeric liquids, 2nd Ed. John Wiley Sons, New York, Toronto 2:105
33. Bestul AB (1956) J Chem Phys 24:1196
34. Ballauff M, Wolf BA (1988) Adv Pol Sci 85:1
35. Wolf BA (1987) Makromol Chem Rapid Comm 8:461
36. Odell JA (1990) private communication
37. Keller A, Odell JA (1985) Colloid Polym Sci 263:181

Received July 6, 1990;
accepted January 17, 1991

Authors' address:

Dr. T. Q. Nguyen
Ecole Polytechnique Fédérale
Dept. des. Matériaux
Laboratoire des Polymères
32, Chemin de Bellerive
1007 Lausanne, Switzerland